

Early Detection of Melanoma using Optimized Segmentation-based CNN Classification

¹Mr. Muthukumar Palani, ²Dr. Velumani Thiyagarajan

Submitted: 28/01/2024 Revised: 06/03/2024 Accepted: 14/03/2024

Abstract: Skin cancer is among the most dangerous types of cancer, posing a significant threat to global mortality rates. Initial recognition is crucial in reducing the fatalities linked to this disease. However, the traditional diagnostic approach, which relies on visual inspection, has limitations in accuracy. This research investigates skin cancer detection and classification by incorporating Deep Learning and image processing tools. The initial step focuses on preprocessing dermoscopic images. To accomplish this, the Dull Razor technique is applied to effectively remove unwanted hair particles from the skin lesion. Subsequently, the Anisotropic Diffusion filter (ADF) is employed to attain image smoothing while preserving image edges. The refinement of the ADF is achieved by incorporating the Mayfly Optimization (MFO) algorithm to optimize gradient weight samples. Segmentation of the preprocessed skin images is carried out using the Active Contour Method (ACM), followed by morphological post-processing to refine the segmented output. The subsequent stage entails the utilization of the ALO algorithm to extract and select optimal features, ultimately enhancing classification accuracy. The culmination of this process involves the classification of chosen features using a CNN with ReLU activation function. The experimental analysis conducted on the Dermnet dataset, comprising nine distinct dermoscopic image types, yields an impressive accuracy rate of approximately 98.25%.

Keywords: Mayfly Optimization (MFO), Active Contour Method (ACM), Ant Lion Optimization (ALO), Convolutional Neural Network (CNN) with Rectified Linear Unit (ReLU).

1. Introduction

Globally, there has been a discernible rise in the prevalence of skin cancer in recent decades, which may be related to alterations in social and lifestyle practices and the ozone layer's thinning. One in six Americans will at some point in their lives develop skin cancer, one of the most prevalent forms of cancer, which is essentially defined by abnormal skin cell growth. It makes up one-third of all cancer cases in the US, and malignant melanoma is almost exclusively to blame for the roughly 75% of deaths associated with the disease. Skin cancer risk factors include individuals with hereditary cancer genes, those with pre-existing lesions, and people who have been exposed to sunshine or radiation for an extended period of time. Melanoma, squamous cell carcinoma, and basal cell carcinoma are the three primary forms of skin cancer. It is commonly known that basal cell carcinoma is frequently treatable. If left untreated, squamous cell carcinoma has the potential to spread quickly and aggressively to other body areas. The most dangerous type of skin cancer, melanoma, can be fatal and manifest with signs including bleeding or seeping.

Non-melanoma, the more common type, has a

comparatively lower mortality rate. Despite the observed increase in skin cancer incidence, diagnosis remains challenging, even for dermatologists. Prompt diagnosis is essential in identifying the condition and obtaining suitable treatment, thereby elevating the survival rate to 94%. Dermatologists typically conduct disease screening using visual inspection, followed by a biopsy. Nevertheless, even proficient dermatologists have a success rate of less than 80% in accurately identifying cancer cells. As a result, computer-assisted image analysis algorithms are utilized to facilitate early detection of the condition. As a result, there is a growing interest in integrating computer-aided methodologies to support medical professionals in their decision-making processes [Shamsi et al, 2021].

2. Literature Work:

The author introduced a ResNet50 CNN model trained using clinical images. The study aimed to distinguish between melanoma and atypical nevi. Initially, the model underwent training with a limited dataset consisting of 20 melanomas and 100 nevi, which was subsequently expanded to 402 melanomas and 402 nevi due to the initial sample size's inadequacy. The results indicated notable enhancements in performance compared to evaluations conducted by 157 board-certified dermatologists. Tests outlined in this study revealed that the trained model achieved accuracy on par with 145 dermatologists while demonstrating improved sensitivity.

In this, the authors delved into the challenges associated with transferring learned features across different races. They highlighted findings from where a

1Ph. D Research Scholar, Department Computer Science, Rathinam College of Arts and Science (Autonomous), Coimbatore. -21

2Assistant Professor & Head Department of IT, Rathinam College of Arts and Science (Autonomous), Coimbatore. -21, Velumani46@gmail.com

model trained predominantly on Asian skin yielded inferior results when applied to white skin. Additionally, the authors explored transfer learning in melanoma cancer classification, demonstrating that retraining pre-existing models not only saves time but also enhances performance. Their experiments involved comparing various state-of-the-art ConvNets to identify the most effective model for melanoma detection.

The authors of this work used a dataset that included over 100,000 benign skin lesions and melanoma cases to train an Inception V4 model. Even with insufficient data, the DL model showed significantly greater mean specificity when compared to dermatologists.

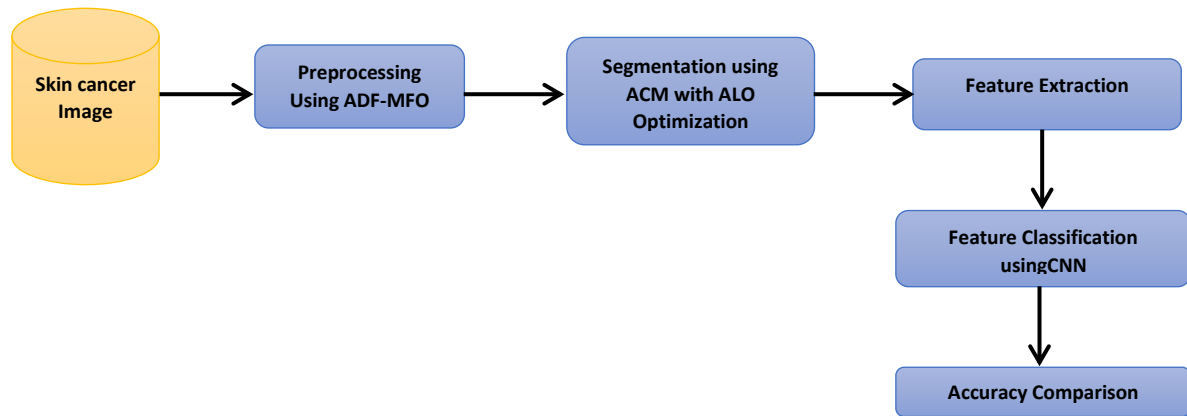


Fig 1: Overall Methodology of Skin cancer Detection and Classification

3.1. Pre-Processing

The pre-processing method aims to eliminate undesired noise and enhance images through the application of image processing techniques, encompassing actions such as smoothing and sharpening.

The primary goal of this stage is to enhance the quality of the melanoma image by removing unnecessary and unconnected elements from the background, thereby preparing it for subsequent processing stages. The initial step in the Image Processing approach for Skin cancer identification involves the implementation of the Dull Razor Technique, which effectively removes coarse hair from the skin region. Subsequently, after this hair removal process, the next step in preprocessing entails the utilization of the Anisotropic Diffusion Filter, commonly referred to as Perona–Malik diffusion. The objective of this technique is to diminish image noise while conserving vital elements of the image's content, such as edges, lines, and other important details crucial for interpreting medical images .

Anisotropic diffusion is defined as

$$\frac{\partial I_m}{\partial t} = \text{div}(q(e, f, l)\nabla I_m) = \nabla q \cdot \nabla I + c(e, f, l)\Delta I_m \quad (1)$$

Where,

3. System Design

In this section, we explore the use of deep learning methods for skin cancer identification. Automated recognition of various skin cancer types requires the integration of multiple methods in computer vision. An optimization method helps identify important skin traits, while deep learning techniques are used for categorization. The Convolutional Neural Network (CNN) leverages the extracted feature vectors to classify an individual's melanoma cancer. A comprehensive illustration of the Skin Cancer Detection and Classification process is depicted in Figure 1.

Δ denotes the Laplacian, ∇ denotes the gradient, $\text{div}(\dots)$ is the divergence operator and $q(e, f, l)\Delta$ is the diffusion coefficient.

For $l > 0$ the output image is available as $I_m(\cdot, l)$, with larger producing blurrier images.

$q(e, f, l)$ regulates the diffusion rate and is typically selected based on the image gradient to retain edges in the image.

$$c(\|\nabla I_m\|) = e^{-\left(\frac{\|\nabla I_m\|}{l}\right)^2} \quad (2)$$

Based on the discrete sampled image, the equation made by Perona and Malik [20] [21] as follows:

$$I_m^{t+1} = I_m^t + \frac{\Delta t}{|\rho^L|} \sum_{a \in \rho} g(|\nabla I_{m,L,a}(t)|) \nabla I_{m,L,a}(t) \quad (3)$$

Where, t represents the discrete time, I_r^t is the discrete image sample, ρ^L is neighbourhood pixel k , $|\rho^L|$ gives the count of neighbouring pixels. The image gradient magnitude for the given direction is described by the given formula as:

$$\nabla I_{m,L,a}(t) = I_m^t - I_{m,L}^t, a \in \rho^L \quad (4)$$

3.2. Segmentation

Image segmentation stands as a focal point within the realms of image processing and computer vision. Moreover, it serves as a fundamental underpinning for image recognition. This technique

operates on specific criteria to partition an input image into several homogeneous categories, thereby facilitating the extraction of areas that hold human interest. This process forms the bedrock for image analysis and the comprehension of both feature extraction and recognition within images.

3.2.1. Active Contour Method (ACM):

The term Active Contour Model often referred to as a "Snake" as demonstrated [22], pertains to a spline that minimizes energy. This spline is directed by external constraints and responsive to image forces that draw it towards distinct features like lines and edges [23]. The configuration of the snake can be depicted using a collection of points $S(a, b) = (m(a, b), n(a, b))$ on melanoma image parameter relating $top \in [0,1]$.

The energy function can be written as:

$$E_{snake} = \int_0^1 E_{int}(v(s)) + E_{ext}(v(s)) ds \quad (5)$$

Upon nearing the boundary position of the object, the external energy of the snake, the gradient of the image is computed by

$$E_{ext} = E_{img} + E_{con} \quad (6)$$

The Internal Energy can be calculated using

$$E_{int} = E_{cont} + E_{curv} \quad (7)$$

Where $E_{cont} \rightarrow$ snake's stability and $E_{curv} \rightarrow$ snake's elastic degree.

$$E_{cont} = \alpha (s) |v_s(s)|^2 \quad (8)$$

$$E_{curv} = \beta (s) |v_{ss}(s)|^2 \quad (9)$$

One of the challenges faced by active contour models is their susceptibility to the precise position of the contour within local minima. When dealing with larger problem sizes, substantial computational resources are consumed. Addressing this issue involves the utilization of the ALO optimization algorithm.

3.2.2. Algorithm: ACM with ALO optimization:

Inputs: $S(p, q), E_{int}, E_{ext}, t$

Output: Segmented region of Melanoma region

Method:

1. To approximate the preferred contour's position and shape by representing it as a curve within the provided image pixels.
2. Initialize the E_{int} and E_{ext} using the equation

3. The energy function can be calculated as
 - a. The optimal weight value of the energy can be obtained using ALO algorithm
 - b. Compute the weights using ants and antlion population at randomly.
 - c. Estimate the fitness function
 - d. Discovering efficient antlion species and implementing them as the optimal choice.
 - e. When the last requirement is not satisfied,
 - f. Use the roulette wheel to select the antlion for each ant.
 - g. Update c^t and d^t using the equation Equations
 - h. build the random walk and normalize it using Equations
 - i. Use equation to update the ant's position.
 - j. Determine and Update Every Ant's Fitness
 - k. If a new ant has a higher fitness level than the old one, it replaces the old one using equation
 - l. If an antlion achieves a higher level of fitness than the current elite, the elite is revised.
 - m. End while
 - n. Update the best weight value
 - o. Compute the total energy
 - p. Modify the pixels to minimize the overall energy
4. The segmentation of ACM has been improved using the weight minimized in the energy function
5. Display the segmented region of Melanoma image.

3.3 Feature Classification

The classification and feature extraction functions of the CNN are carried out using the ReLU, which is an activation function. It features two main phases: the learning phase and the classification phase. The latter involves pooling and convolution layers. The CNN helps in simplifying the categorization process by allowing users to understand visual features more easily

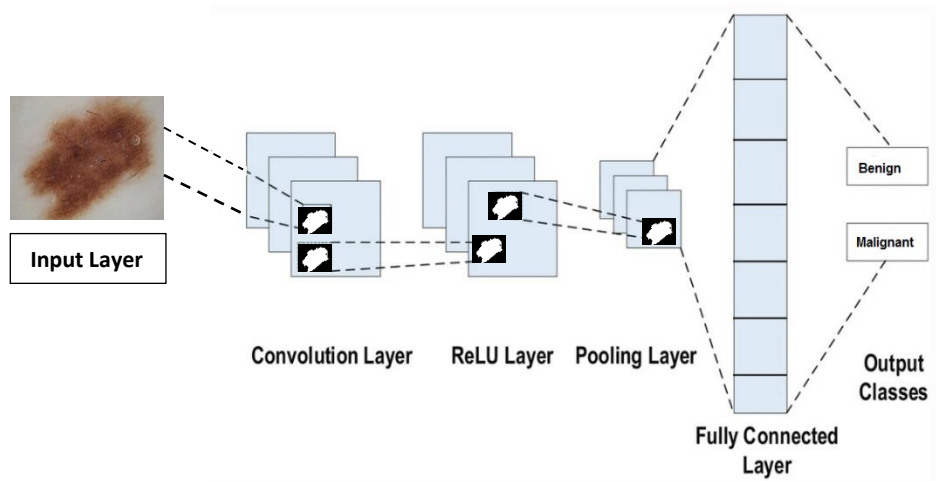


Fig 2: Architecture of CNN

Convolutional Layer:

Several filters iterate through the input data in the convolution layer, multiplying each element by itself to determine the total. The input's receptiveness grade is determined by evaluating the resultant output. The value of the weighted summation is an input for the layer that comes next. A sliding focus region fills in the values for extra pixels in the convolutional layer's output. Moreover, each convolution layer action has zero padding, stride, and filter size conditions linked to it.

4.1. Dataset Description

We gathered over 400 sample images from both the Kaggle Website and the Dermnet dataset to detect early-stage Melanoma Cancer. The dataset comprises two classes: 1. Benign and 2. Malignant. Employing our innovative DCNN Classification approach, we utilized 250 image samples for training and 150 image samples for testing the model.

4.2. Performance Measures

We assess the performance of the DCNN method in contrast to prevailing methods such as Adaptive Neuro Fuzzy Inference System (ANFIS), Fuzzy Neural Network (FNN), and Fuzzy Neural Network with Jaya Optimization (FNN-JO). We measure their effectiveness

using performance metrics including F-Measure, Recall, Specificity, Accuracy, and Precision.

$$\text{Precision} = \frac{TP}{(TP + FP)} \quad (10)$$

$$\text{Recall} = \frac{TP}{(TP + FN)} \quad (11)$$

$$\text{Specificity} = \frac{TN}{(TN + FP)} \quad (12)$$

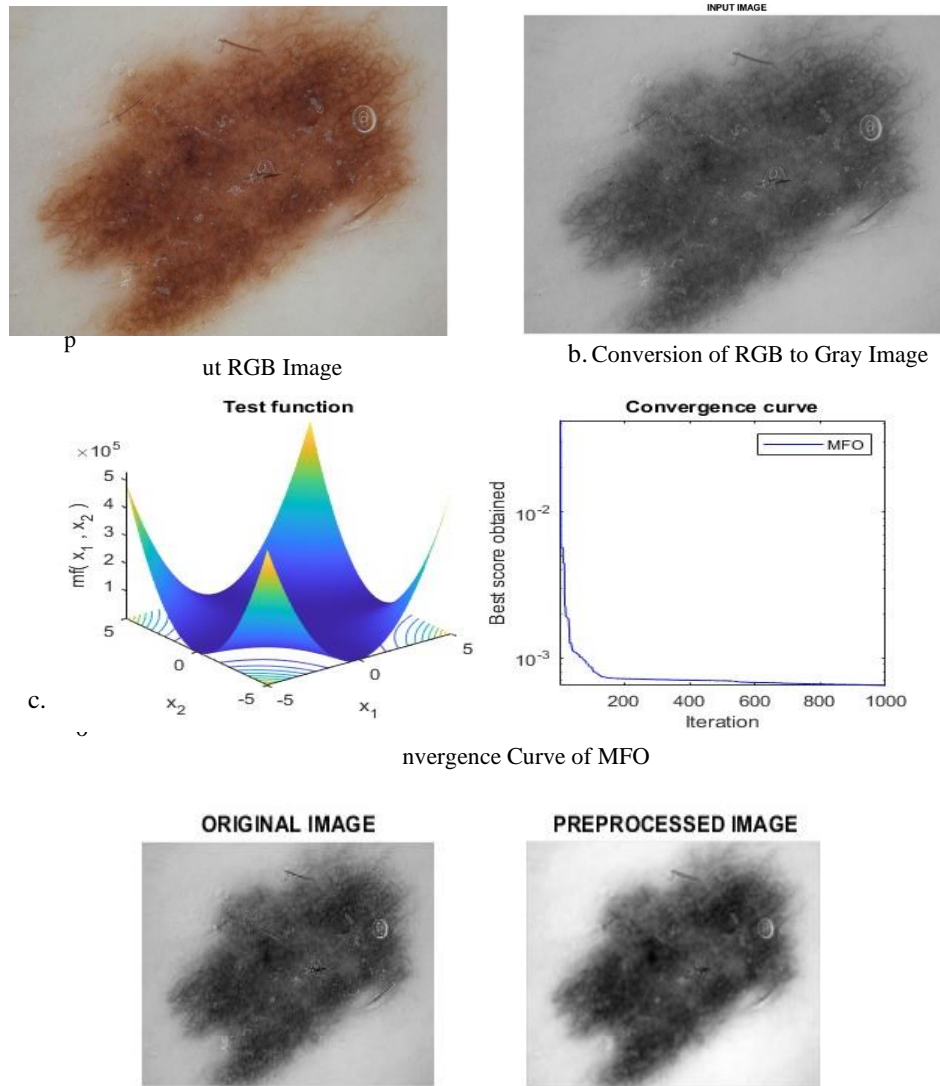
$$\text{Accuracy} = \frac{(TP+TN)}{(TP+FN+TN+FP)} \quad (13)$$

$$\text{F-Measure} = 2 * \frac{\text{Precision} * \text{Recall}}{\text{Precision} + \text{Recall}} \quad (14)$$

4.3. Performance Estimation

The pre-processed picture is improved, and key features are extracted via feature selection and segmentation. The classification performance of the DCNN is compared to an existing method. The categorization stage then receives this extracted data. The model uses a learning rate of 0.016 and a drop factor of 0.1 with a batch size of 128 and stochastic gradient descent with momentum optimization. In order to store the pertinent features and the labels associated with skin cancer, it also uses eight channels in the batch-normalized layer and nine classes in the fully linked layer.

4.3.1. Preprocessing: Anisotropic Diffusion Filter (ADF) and Mayfly Optimization (MFO) has been used in this study to preprocess the images. The figure 3 shows the preprocessing image results.



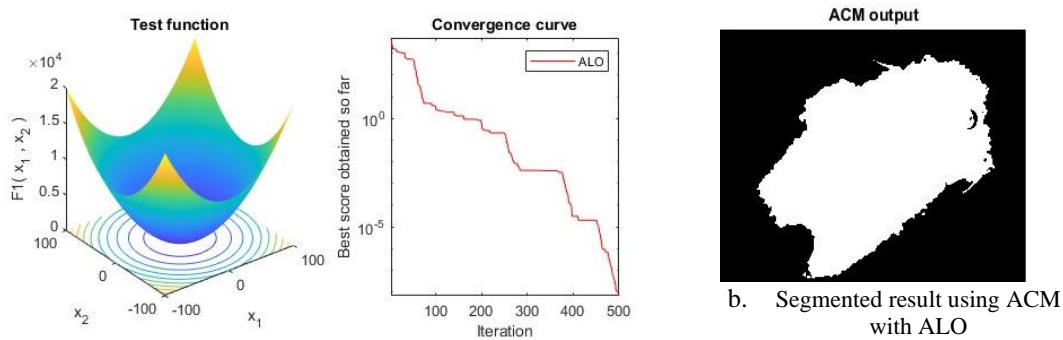
d. Preprocessed Image using ADF with MFO
Fig 3: Preprocessed Image results

4.3.2. Segmentation: To improve accuracy and optimize the classification of skin cancer within the image, the segmentation process becomes necessary. In this article, Active contour method (ACM) with Ant Lion optimization (ALO) was utilized for getting the accurate results of segmentation.

To enhance prediction accuracy, the complete segmentation of skin cancer images is performed on preprocessed images using the ALO algorithm within framework of Active Contour Model (ACM). ALO optimizes the weight values employed in ACM, generating the optimal score for segmented images. Inspired by the foraging behavior of Ant lions, ALO offers

various advantages, including user-friendliness, scalability, flexibility, and a balance between exploration and exploitation.

Utilizing ACM with ALO, the scheme effectively segments the pertinent region within the entire skin cancer image, and subsequent morphological post-processing steps strengthen the accuracy of the proposed approach. Consequently, this process yields optimal features extracted from the segmented image region, thereby simplifying the training process for the Deep Convolutional Neural Network (CNN) classifier. The figure 4.a and 4.b shows the convergence curve of ALO and the final segmented result respectively.



a. Convergence Curve of ALO
Fig 4: Outcome of Segmentation Result using ACM with ALO

4.3.3. Classification of Skin Cancer

A Deep CNN with the RELU as an activation function has been utilized. Based on the outcome of the ROI of segmented region of skin cancer using ACM with ALO, classification accuracy has been improved and achieved

the progress of the result as 100%. The figure 5 shows the accuracy and loss function of the Deep CNN.



Fig 5: Accuracy and Loss function of the Deep CNN.

With the aid of optimized weights used in preprocessing and segmentation using MFO and ALO respectively to produce the better features

for determining the type of skin cancer. Table 1 and Figure 5 shows the Classification recital of Deep CNN.

Table 1: Comparison of Skin cancer Classification

Performance Measures	Proposed Deep CNN	FNN-JO	FNN	ANFIS
Accuracy (%)	100	89	76	61
Specificity (%)	88.36	80.13	61.92	40.53
Precision (%)	90.15	71.26	65.22	34.33
Recall (%)	96.41	72.69	53.48	42.51
F-measure (%)	86.34	74.12	66.48	30.17

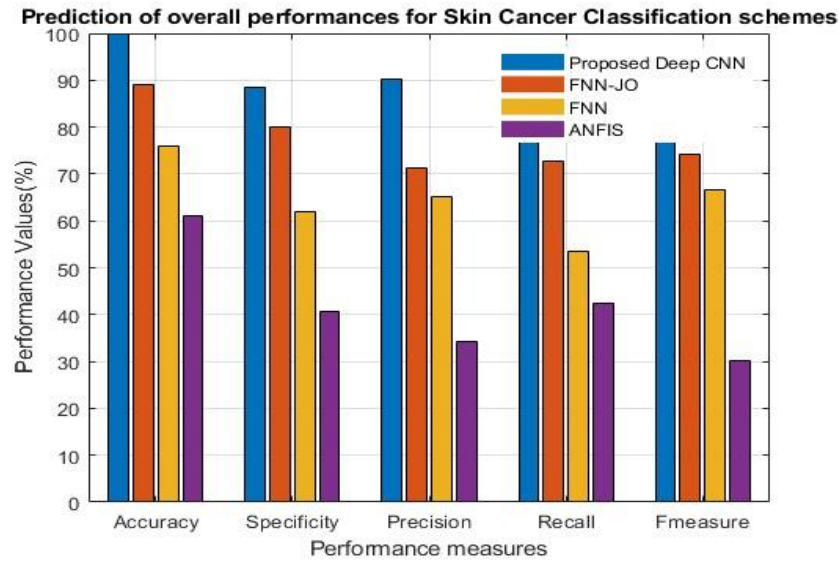


Fig. 6 Forecasting the overall performance of skin cancer classification methods.

Figure 5 illustrates a comparison of skin cancer categorization effectiveness between the proposed Deep CNN and other existing classifiers. The suggested method demonstrates a classification accuracy that is on par with the other classifier, with Deep CNN outperforming FNN-JO, FNN, and ANFIS by 11%, 24%, and 39%, respectively. Moreover, the classification specificity of the suggested Deep CNN approach surpasses RF, FNN-JO, FNN, and ANFIS by 8%, 26%, and 48%, respectively. Additionally, the classification precision of Deep CNN exceeds that of FNN-JO, FNN, and ANFIS by 19%, 25%, and 56%, respectively. Furthermore, the proposed Deep CNN approach exhibits a higher classification recall compared to FNN-JO, FNN, and ANFIS by 24%, 43%, and 54%, respectively. Finally, the classification f-measure of the suggested Deep CNN approach exceeds that of FNN-JO, FNN, and ANFIS by 12%, 20%, and 56%, respectively. In conclusion, the suggested Deep CNN demonstrates superior classification performance compared to the current method.

5. Conclusion

This paper presents a novel approach to identifying melanoma skin cancer with DCNN classification. Initially,

References

- [1] Jerant AF, Johnson JT, Sheridan CD, Caffrey TJ (2000) Early detection and treatment of skin cancer. *Am Fam Physician* 62(2):357–368
- [2] Khaledyan D, Tajally A, Sarkhosh A, Shamsi A, Asgharnezhad H, Khosravi A, Nahavandi S (2021) Confidence aware neural networks for skin cancer detection. *arXiv preprint arXiv:2107.09118*
- [3] Rehman A, Naz S, Razzak I (2021) Leveraging big data analytics in healthcare enhancement: trends, challenges and opportunities. *Multimed Syst* 1–33:1339–1371
- [4] Razzak MI, Imran M, Xu G (2020) Big data analytics for preventive medicine. *Neural Comput Appl* 32(9):4417–4451
- [5] Shamsi A, Asgharnezhad H, Jokandan SS, Khosravi A, Kebria PM, Nahavandi D, Nahavandi S, Srinivasan D (2021) An uncertainty-aware transfer learning-based framework for covid-19 diagnosis. *IEEE Trans on Neural Netw and Learning Syst* 32(4):1408–1417
- [6] Brinker, T. J., Hekler, A., Enk, A. H., Klode, J., Hauschild, A., Berking, C., ... Frohling, S. (2019). A convolutional neural network trained with dermoscopic images performed on par with 145 dermatologists in a

- clinical melanoma image classification task. *European Journal of Cancer*, 111, 148–154. doi:10.1016/j.ejca.2019.02.005
- [7] Goyal, M., Knackstedt, T., Yan, S., & Hassanpour, S. (2020). Artificial intelligence-based image classification methods for diagnosis of skin cancer: Challenges and opportunities. *Computers in Biology and Medicine*, 127, 104065. doi:10.1016/j.compbiomed.2020.104065
- [8] Sagar, A., & Dheeba, J. (2020). Convolutional neural networks for classifying melanoma images. Cold Spring Harbour Laboratory. bioRxiv. doi:10.1101/2020.05.22.110973
- [9] Haenssle, H. A., Fink, C., Schneiderbauer, R., Toberer, F., Buhl, T., Blum, A., ... Uhlmann, L. (2018). Man against machine: Diagnostic performance of a deep learning convolutional neural network for dermoscopic melanoma recognition in comparison to 58 dermatologists. *Annals of Oncology : Official Journal of the European Society for Medical Oncology*, 29(8), 1836–1842. doi:10.1093/annonc/mdy166 [Crossref] [PubMed] [Web of Science ®], [Google Scholar]
- [10] Haenssle, H. A., Fink, C., Toberer, F., Winkler, J., Stolz, W., Deinlein, T., ... Zutt, M. (2020). Man against machine reloaded: Performance of a market-approved convolutional neural network in classifying a broad spectrum of skin lesions in comparison with 96 dermatologists working under less artificial conditions. *Annals of Oncology : Official Journal of the European Society for Medical Oncology*, 31(1), 137–143. doi:10.1016/j.annonc.2019.10.013
- [11] Adegun, A., & Viriri, S. (2021). Deep learning techniques for skin lesion analysis and melanoma cancer detection: A survey of state-of-the-art. *Artificial Intelligence Review*, 54(2), 811–841. doi:10.1007/s10462-020-09865-y
- [12] Akkoca-Gazioğlu, B. S., & Kamasak, M. (2020). Effects of objects and image quality on melanoma classification using deep neural networks. *Biomedical Signal Processing and Control*, 67, 102530. doi:10.21203/rs.3.rs-35907/v1
- [13] Jojoa Acosta, M. F., Caballero Tovar, L. Y., Garcia-Zapirain, M. B., & Percybrooks, W. S. (2021). Melanoma diagnosis using deep learning techniques on dermoscopic images. *BMC Medical Imaging*, 21(1), 6. doi:10.1186/s12880-020-00534-8
- [14] Dildar, M., Akram, S., Irfan, M., Khan, H. U., Ramzan, M., Mahmood, A. R., ... Mahnashi, M. H. (2021). Skin cancer detection: A review using deep learning techniques. *International Journal of Environmental Research and Public Health*, 18(10), 5479. doi:10.3390/ijerph18105479